Int. J. Solids Structures Vol. 26, No. 5/6, pp. 601–615, 1990
Printed in Great Britain.

0020–7683/90 $3.00 + .00

COLLAPSE OF A LATERALLY COMPRESSED SQUARE TUBE RESTING ON A FLAT BASE

N. K. GUPTA
Department of Applied Mechanics, IIT-Delhi, Huaz Khas, New Delhi, 110 016, India

and

S. K. SINHA
SEMAC PVT Ltd, Consulting Engineers, B-6/23 Safdarjung Enclave,
New Delhi 110 029, India

(*Received* 8 *February* 1989; *in revised form* 17 *July* 1989)

Abstract—Square tubes of aluminium and mild steel, placed on a rigid flat surface, were compressed by wedge-shaped and flat-faced indenters of short width in an Instron machine. Their collapse behaviour under different indenters was studied and typical histories of their deformation and load–compression response are discussed. A simplified analysis, which considers the formation of stationary and travelling hinges and employs certain assumptions based on the experimental results, is presented for the description of the collapse behaviour of the tubes. The results obtained thereby have been compared with the experimental results.

NOTATION

H, X	height and width of the tube, see Fig. 9(a)
L, Lo	length of tube and its overhang
M_P	plastic moment per unit length
P	lateral load
r	radius of a travelling hinge
S	area swept by a travelling hinge
W	width of platen
W_{AB} etc.	energy absorbed at hinge AB, etc.
α_{AB} etc.	angle of rotation of a stationary hinge AB, etc., Fig. 9
δ	compression or relative indenter movement
σ_0	yield stress.

1. INTRODUCTION

Studies in axial and lateral collapse of tubes are important for these find application (Ezra and Fay, 1972; Johnson and Reid, 1978) in energy absorbing devices and in relation to crashworthiness. Axial compression of round or square tubes (Jones and Abramowicz, 1985), and lateral compression of round tubes (Reid, 1983) have received much attention in recent years. Studies available in the lateral compression of square rings or tubes (Sinha and Chitkara, 1982; Gupta and Sinha, 1989) have mostly considered the collapse due to symmetrically placed opposing indenters. An attempt is made here to study the plasto mechanics of a deforming tube which rests on a flat base and is compressed (Sinha, 1988) from the other side by a wedge-shaped or a flat-faced indenter of short width, see Fig. 1(a).

Experiments were performed on aluminium and mild steel tubes and results obtained for their history of deformation as well as load and energy versus compression curves are presented here and the influence thereon of different parameters is discussed. A simple theoretical model, which considers the formation of stationary and travelling plastic hinges and employs assumptions based on experimental results, is presented for the analysis of the tube collapse behaviour. The energy absorbed and the load compression characteristics of the tubes during the collapse are computed and results thus obtained have been compared with the experiments.

2. EXPERIMENTS

Square tubes of aluminium and mild steel of dimensions given in Table 1, were obtained commercially in 3.5 m length each, and were later cut to different lengths as required in different experiments.

Aluminium tubes were tested in as received condition, while mild steel tubes were tested in both as received and annealed conditions. Mild steel tubes were annealed by soaking them at 900°C for 30 min before allowing them to cool in the furnace for 24 h.

The tubes were tested in a 50 T Instron machine at a speed of the crosshead movement of 2 mm per minute. The indenters used in these tests were either flat-faced, of width 4 mm, 24 mm and 46 mm, or wedge-shaped, of 60° or 120° angle. These were made of hardened die steel and were ground. In all experiments, symmetry of tube placement and alignment of indenter were checked before commencing the compression. The load compression graphs were obtained on the automatic chart recorder of the machine. During compression, the deforming shape of a specimen was studied and photographed by interrupting the test at different stages.

3. RESULTS AND DISCUSSIONS

The deformation of the tube was seen to be unsymmetrical with respect to the horizontal mid plane between the indenters. Figure 1(b) shows different stages of a 24 mm size aluminium tube compressed by a 24 mm wide flat indenter, and Fig. 1(c) illustrates the final deformed shapes in the case of steel tubes of 24 mm and 37 mm size, compressed by a 60° wedge. The plastic deformation in the tube was seen to be most predominant in the region under the direct load, but it decreased gradually with distance away from the loaded zone. If the tube is sufficiently long ($L \geqslant W+3H$), the tube remains completely undeformed beyond a distance (H to 1.1 H) from the edge of the loaded zone. The portions of the tube which remain undeformed begin to bend inward towards the indenter and undergo a rigid body movement.

3.1. *Lateral compression by a wedge*

Wedges used in these tests were of 60° and 120° angles. In the initial stage of the test, there is a local indentation in the portion of the tube which is directly under the wedge, followed by bulging out of the vertical sides. The maximum bulge is seen to be close to the wedge. These bulges then take the form of plastic hinges of finite length which begin to travel as further compression is continued. Load compression curves for 24 mm and 35 mm size aluminium tubes are shown in Figs 2(a) and 2(b) respectively. Figure 2(a) shows results of a typical test on 24 mm size aluminium tube superposed for 60° and 120° wedges. Compared to the 60° wedge, the 120° wedge results in a higher initial peak load and the load compression curves in both the cases merge with the fall of the load. But as compression is continued, the P-δ curve for the tube, under the 120° wedge, rises more steeply than the corresponding curve for the 60° wedge. This is due to the fact that the deforming tube walls which are bending inwards, touch the sides of the 120° wedge indenter earlier on in the test. The tube, however, deforms symmetrically with respect to the vertical longitudinal mid

Table 1. Dimensions of tubes

Material	Size (mm^2)	Thickness (mm)
Aluminium	24	1.0
	35	1.1
	50	1.2
Mild steel (as recd.)	24	1.0
	37	1.0
Mild steel (annealed)	24	1.0
	37	1.0

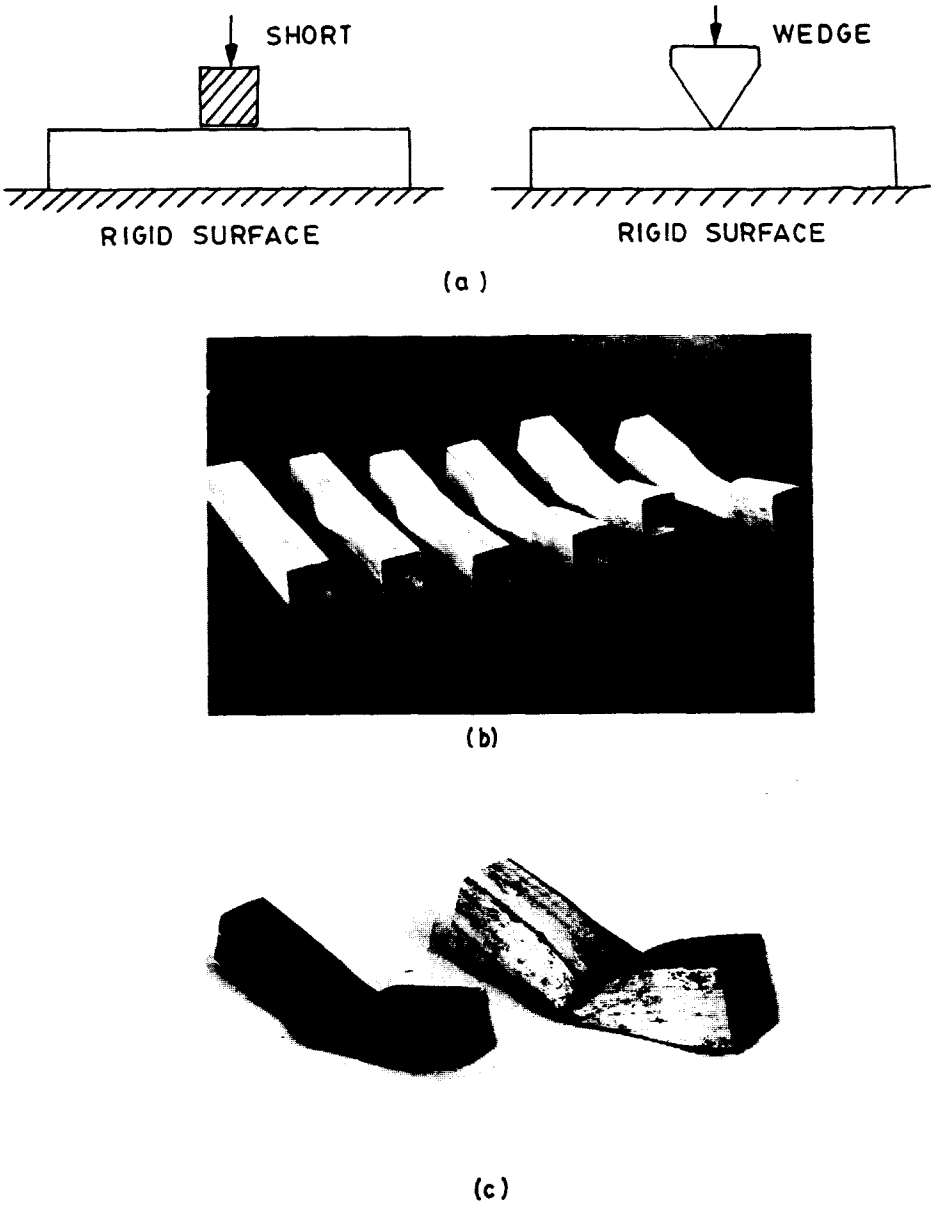

Fig. 1. Compression of a tube placed on a rigid surface, (a) schematic diagram, (b) different stages of compression in the case of 24 mm aluminium tube under 24 mm platen, and (c) final deformed shapes of 24 and 35 mm steel tubes under 60° wedges.

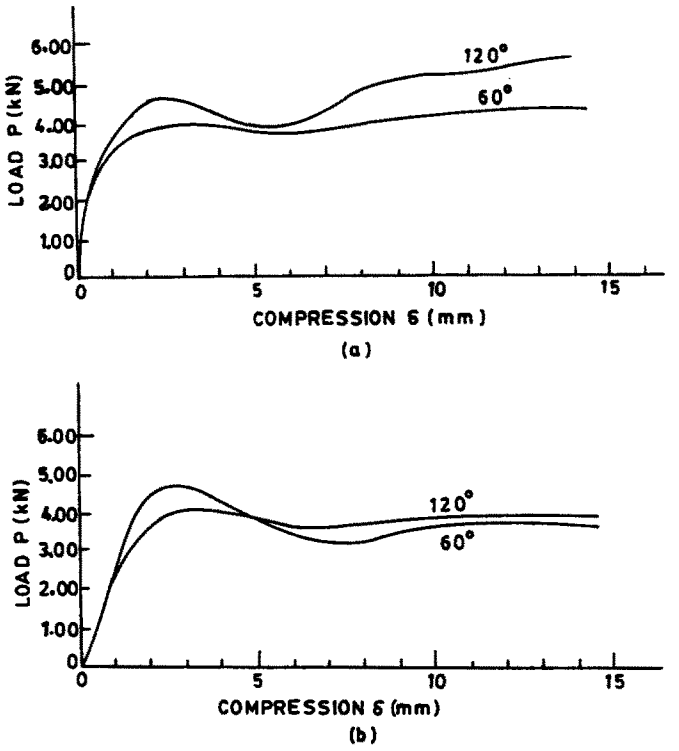

Fig. 2. Load compression curves under a wedge for (a) 24 mm and (b) 35 mm aluminium tubes. Curve for 120° wedge (b) is typical for a tube which became rhomboidal.

plane in both the cases. Some typical load deformation curves for mild steel tubes are shown in Fig. 3(a) for 24 mm size tube in as received and annealed conditions and in Fig. 3(b) for 37 mm size tube in as received condition. The sequence of deformation in these cases is quite similar to that of 24 mm size aluminium tubes. In a few tests, however, the tube deformation was accompanied by the shifting of its upper face laterally with respect to its bottom face and as a result the square cross section became rhomboidal. One such case was a 35 mm size aluminium tube under 120° wedge. Its load compression graph is shown in Fig. 2(b), wherein it is seen that the rise in load subsequent to the first drop is quite small as compared to the corresponding rise of load in a normal case, as shown in Fig. 2(a).

3.2. *Lateral compression by a 4 mm wide indenter*

A 4 mm thick steel plate of 50 mm height and 150 mm length was welded to a plate to form a right angled Tee. Different square tubes were compressed between a rigid flat base and this Tee. Reason for such a choice was to study the load compression characteristics for lateral compression of a tube in a situation when tube walls would not touch the sides of indenter, as was the case in tests under the wedge-shaped indenters. The load compression curve for 24 mm, 35 mm and 50 mm size aluminium tubes are given in Fig. 4. In this figure we have also superposed (in dotted line) a curve for the 24 mm tube under the 60° wedge, for comparison. Figure 5 shows load compression curves for 24 mm steel tubes in as received and annealed conditions. Here, again, the curve for the 24 mm annealed tube under a wedge of 60° angle is compared with the corresponding curve under the Tee. It is seen that the curve obtained in a test with a 4 mm wide flat indenter shows a drop in load, in comparison with the corresponding curve under 60° wedge at a stage when in the latter case, the tube touches the sides of the wedge.

3.3. *Compression by a flat-faced indenter*

Flat-faced indenters used in the present tests were of 24 mm and 46 mm width, and typical load compression curves obtained in the tests on 24 mm and 50 mm size aluminium

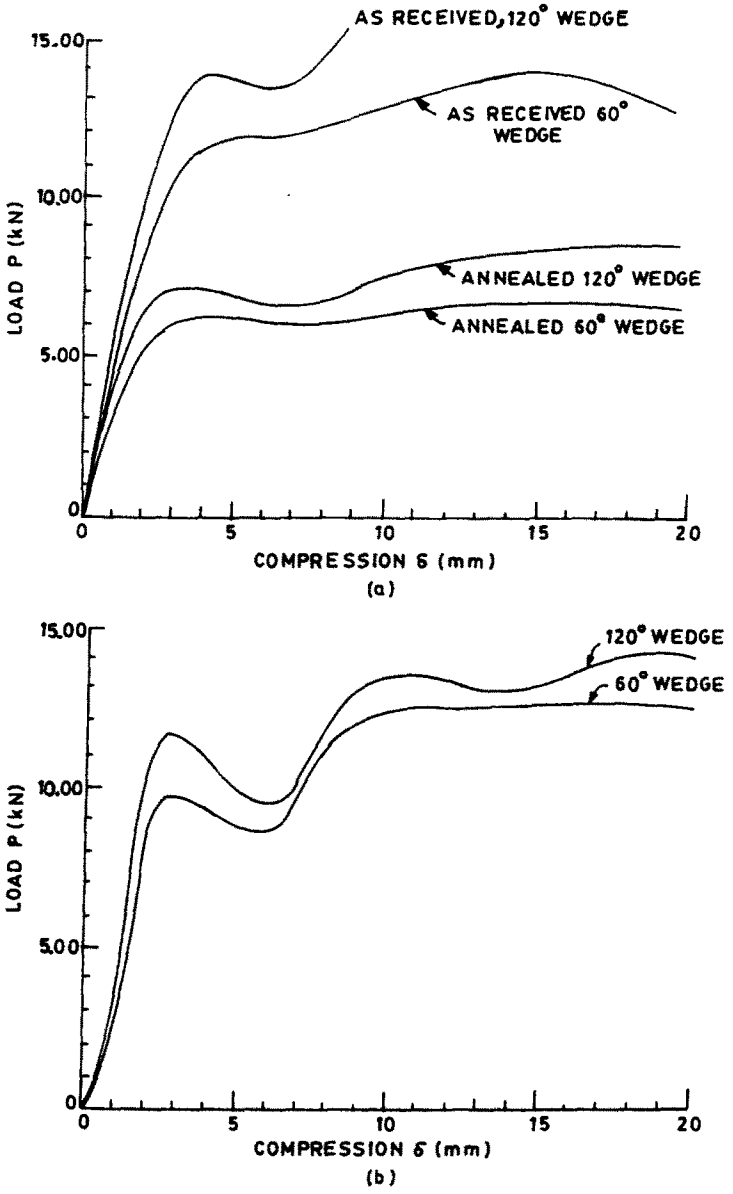

Fig. 3. Load compression curves under a wedge for (a) 24 mm and (b) 37 mm steel tubes.

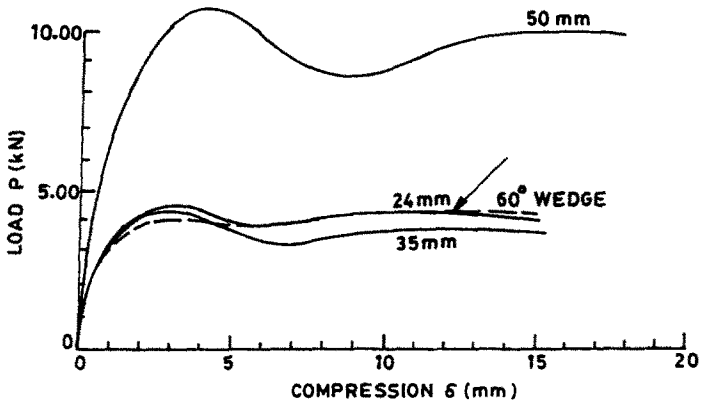

Fig. 4. Load compression curves 24, 35 and 50 mm aluminium tubes under 4 mm wide identer. A typical curve for 24 mm tube under 60° wedge is superposed. Arrow indicates the point when tube begins to touch the wedge.

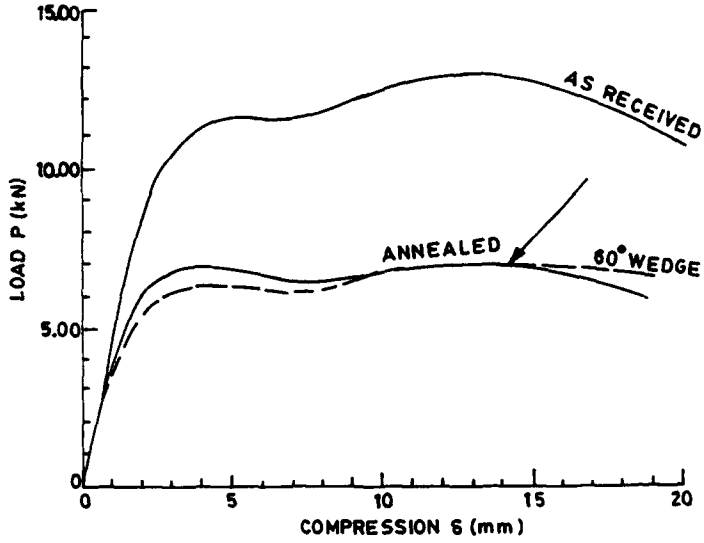

Fig. 5. Load compression curves for 24 mm steel tubes under 4 mm wide indenter. Curve for 60° wedge is superposed in the case of annealed steel. Arrow indicates the point when tube begins to touch the wedge.

tubes of sufficient length ($L \geqslant W+3H$) are shown in Fig. 6. The sequence of deformation in these cases essentially remains the same as described for a wedge. It is, however, seen in these tests that the peak load is followed by a drop in load and a subsequent rise of load once again. The drop in load for the second time continues until the tube ends, which are bending upwards, touch the opposite platen and press against it. The load in the load compression curve begins to rise once again at this stage. Typical results for a 50 mm size

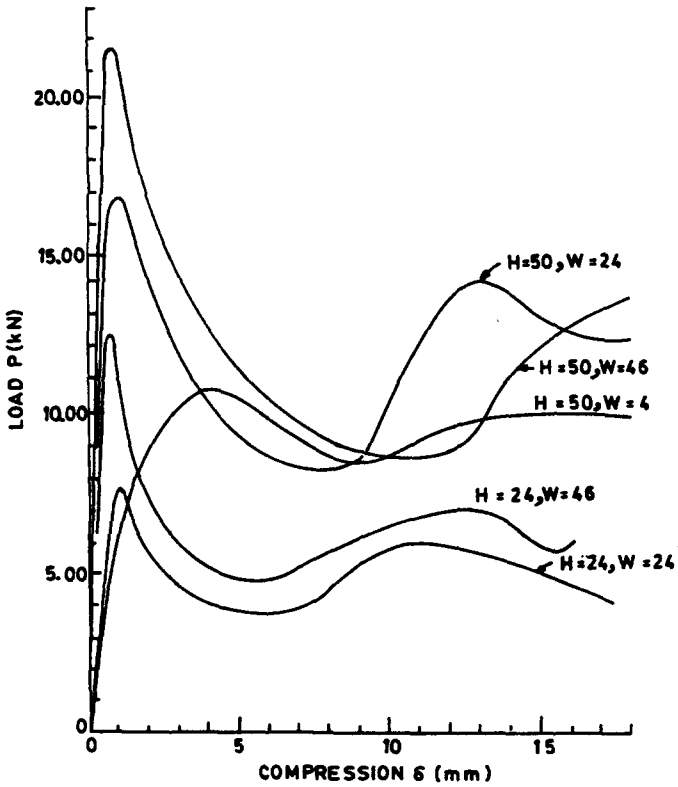

Fig. 6. Load compression curves for 24 and 50 mm aluminium tubes compressed under a 24 or 46 mm wide indenter.

aluminium tube under 24 mm and 46 mm wide indenters are shown in Fig. 6, along with the results obtained under a 4 mm wide indenter. The load compression curves for the tubes, under these indenters, thus seem to oscillate in the post collapse region. For the tubes of shorter lengths, however, the curves are smooth and drop continuously. It is interesting to note that the peak load for a tube increases remarkably with the increase in the width of the platen, while the corresponding variation in post collapse load seems to be relatively much smaller. Further, a variation of the peak load is observed with the increase in length of the tube. Typical results of load compression plots for tubes of different lengths are shown in Fig. 7(a) for 35 mm size aluminium tubes, compressed under a 24 mm wide indenter. Nature of the peak load variation with the length of the tube is shown in the inset of Fig. 7(a). Figure 7(b), however, shows the load compression graphs for a 35 mm size aluminium tube of sufficient length (150 mm), when the indenter width is 4 mm, 24 mm or 46 mm. A curve obtained under a 60° wedge has also been superposed in this figure.

The study of the deformed shapes in the above tests revealed that for a sufficiently long tube, the deformed length in the case of steel specimens, extends beyond the edge of the loaded zone by about 1.1 H; this length in the case of aluminium tubes however is nearly H. Further, the plastic hinges formed in steel tubes have relatively lower curvature.

In all these tests, the tube begins to bend inwards, with its ends leaving the base at some stage of the test. Some experiments were also conducted in which this bending was prevented by clamping the bottom side of the tube with the help of a flat of suitable width. The load compression curves in such a situation are shown in Figs 8(a) to 8(d), for 24 mm size aluminium tubes when compressed under flat-faced or wedge-shaped indenters.

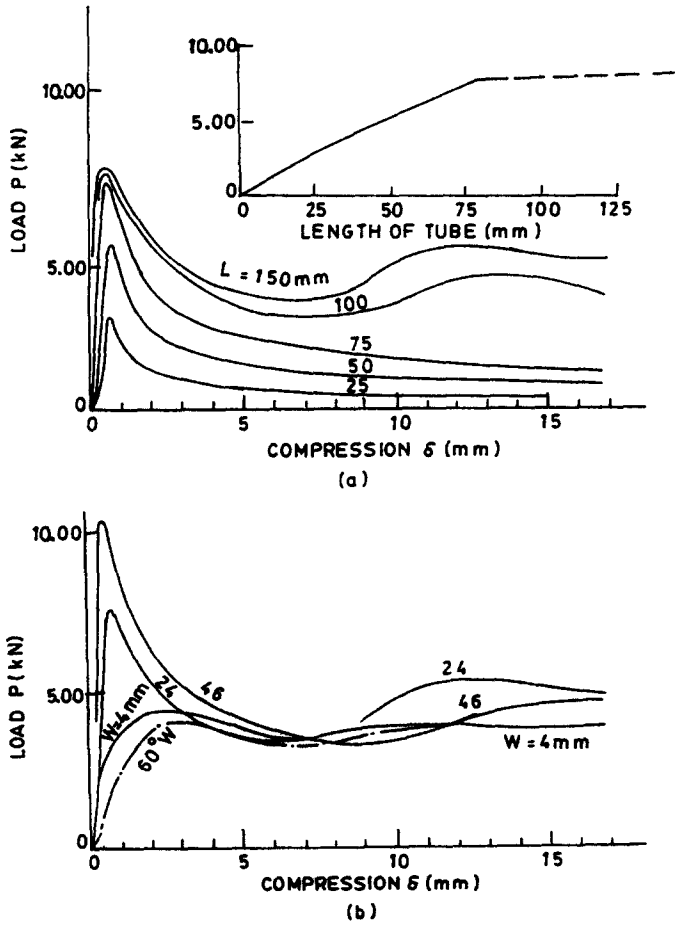

Fig. 7. Load compression curves for 35 mm aluminium tubes compressed under a short flat indenter; (a) tubes of different lengths under 24 mm wide indenter, and (b) indenters of different widths when tube length is kept constant. Inset in (a) shows variation of peak load with tube length.

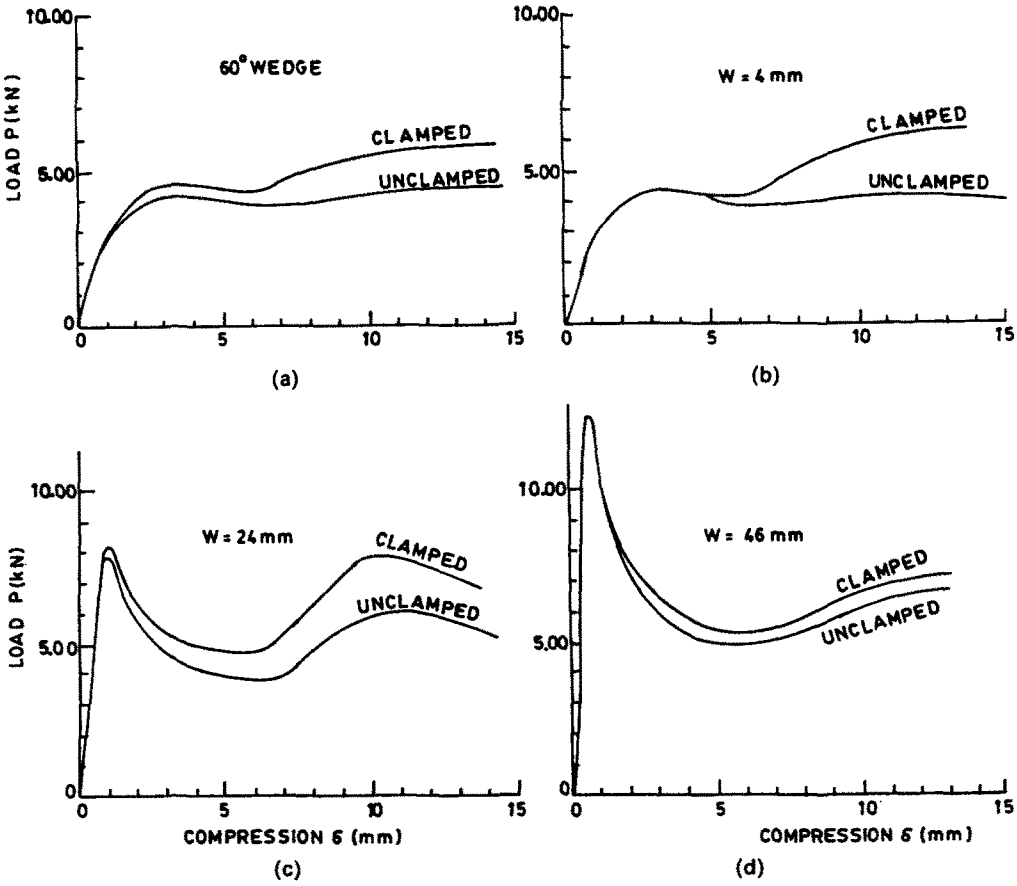

Fig. 8. Load compression curves for 24 mm square aluminium tubes clamped with the full platen and compressed by (a) a wedge; and indenters of (b) 4 mm, (c) 24 mm and (d) 46 mm width.

Corresponding curves for unclamped tubes are also presented for comparison. It is seen that this clamping (i) does not affect the peak load, (ii) increases the affected length, and (iii) results in the higher post collapse load compared to unclamped tubes.

4. ANALYSIS

On the basis of experimental observations discussed above, a simplified collapse mechanism is presented below. It is assumed that all external energy absorbed during the collapse of a tube is consumed in the work done in plastic deformation along stationary or travelling hinges, see Fig. 9.

As mentioned earlier, a bulge is observed on the tube side below the indenter. The shorter the indenter the closer is the bulge to the indenter. As the compression proceeds, this bulge takes the shape of a hinge line, and the angle between the two surfaces meeting at this hinge, becomes smaller and smaller till the hinge almost touches the indenter. At this stage the hinge begins to travel as the test proceeds.

In the final stages of the test, the affected length of the tube (on either side of the indenter) is found to increase gradually up to a maximum, after which it does not increase any further, and the rest of the tube remains practically undeformed. For the purpose of the present analysis, however, it has been assumed that the affected length reaches its maximum right in the beginning of the compression.

For a given indenter movement δ, a set of expressions for angles of rotation of the stationary hinge lines and areas swept by the travelling hinges is derived as follows.

For a given δ, the length of the horizontal line $AB = z$, the distance of the travelling

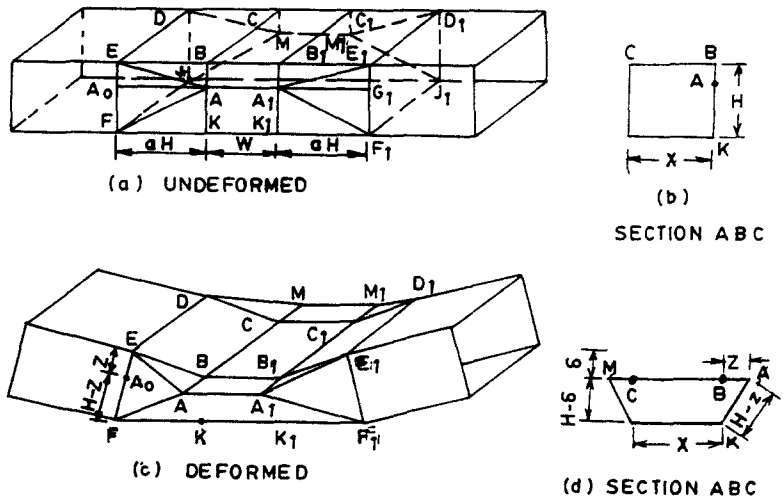

Fig. 9. Deformation mode of a rectangular tube of sufficient length being compressed under a short platen.

hinge AA_1 from the corner BB_1 (Fig. 9a) is given, from the right angled triangle BAK and by assuming inextensibility, as,

$$z^2+(H-\delta)^2 = (H-z)^2$$

or

$$z/H = (\delta/H)(1-\delta/2H)$$

or

$$z = \delta(1-\delta/2H). \tag{1}$$

Here we consider that the length of the tube EB, up to which the deformation extends is $a \cdot H$, where $a = 1$ and 1.1 for aluminium and steel tubes respectively.

Also,

$$A_0A = FK = EB = a \cdot H \tag{2}$$

where A_0 is an imaginary point on EF such that $EA_0 = BA = z$, and $A_0F = H-z$.

Hence,

$$\begin{aligned} A_0B &= (A_0A^2-BA^2)^{1/2} \\ &= ((a \cdot H)^2-z^2)^{1/2}. \end{aligned} \tag{3}$$

The relative rotation of the yield line ED is given by,

$$\alpha_{ED} = \sin^{-1}(z\ a \cdot H) \tag{4}$$

and the energy absorbed in the identical stationary hinges ED and E_1D_1 becomes

$$W_{ED} = 2 \cdot M_P \cdot X \cdot \alpha_{ED} \tag{5}$$

where M_P is the fully plastic moment per unit width of the tube wall, given by $M_P = \sigma_0 t^2/4$.

These equations for the stationary hinges BC (and B_1C_1), FJ (and F_1J_1), EF (and

E_1F_1, DJ and D_1J_1) and BA (and CM, C_1M_1 and B_1A_1) are written as follows:

Rotation of hinge line BC

$$\alpha_{BC} = < EBA_0 + < A_0BF - < BFK$$
$$= \sin^{-1}(EA_0/EB) + \tan^{-1}(A_0F/A_0B) - \tan^{-1}(BK/FK)$$

and

$$W_{BC} = 2 \cdot M_P \cdot X \cdot \alpha_{BC} \tag{6}$$

$$\alpha_{FJ} = \pi/2 - < A_0FB - < BFK$$
$$= \pi/2 - \tan^{-1}(A_0B/A_0F) - \tan^{-1}(BK/FK) \tag{7}$$

$$W_{FJ} = 2 \cdot M_P \cdot X \cdot \alpha_{FJ} \tag{8}$$

$$\alpha_{EF} = \sin^{-1}(BA/A_0A) = \sin^{-1}(z/a \cdot H) \tag{9}$$

$$W_{EF} = 4 \cdot M_P \cdot H \cdot \alpha_{EF} \tag{10}$$

$$\alpha_{BA} = \alpha_{BC}$$

and

$$W_{BA} = 4 \cdot M_P \cdot z \cdot \alpha_{BA}. \tag{11}$$

The corner deformation at EB, E_1B_1 and other identical hinges (DC and D_1C_1) is dealt with by assuming that EB, E_1B_1 etc. must remain straight independently and the rotation about these vary from one full right angle at B to zero E. While BB_1 remains straight and suffers most of the rotation in the beginning, the corner EB deforms in a different manner. It remains straight at E near the undeformed end of the tube and becomes slightly curved at B near the indenter. In what follows, this curvature has been ignored. During the compression, the angle α_{EB} is very small at E, while the same B increases from zero in the beginning to one right angle when the tube is compressed to about one third of its height. This variation is assumed to be linear and an average value of the angle is computed as follows:

$$\alpha_{EB}(\text{av}) = (\alpha_{EB} \text{ at } E + \alpha_{EB} \text{ at } B)/2$$
$$= (\alpha_{EB} \text{ at } B)/2 \tag{12}$$

since α_{EB} at $E = 0$.

Maximum value of $\alpha_{EB}(\text{av}) = \pi/4$ at $\delta/H \geqslant 1/3$.

Similarly it is assumed that α_{BB_1} increases linearly from zero in the beginning to a maximum value of $\pi/2$ at $\delta/H = 1/3$.

Hence,

$$W_{EB} = 4 \cdot M_P \cdot EB \cdot \alpha_{EB}(\text{av}) \tag{13}$$

and

$$W_{BB_1} = 2 \cdot M_P \cdot W \cdot \alpha_{BB_1}. \tag{14}$$

The yield lines AA_1, EA and FA are are seen to be travelling during compression. The energy absorbed by a travelling hinge of radius r in travelling through an area S by bending and unbending (Meng *et al.*, 1983) is given by,

$$dW = 2 \cdot S \cdot M_P/r. \tag{15}$$

The radius of curvature r_0 at the onset of the bulge AA_1 appeared to vary with the variation in the wall thickness and the size of the tube. For the travelling hinges, the following relations seems to fit well with the experimental observations which were made by terminating the tests at about different stages of compression

$$r(\text{of } AA_1) = t \cdot H \cdot (1 - 0.75\,\delta/H) \quad \text{for } r > 1.1t \tag{16}$$

otherwise $r = 1.1(t)$.

Hence,

$$dW(\text{at } AA_1) = 4 \cdot M_P \cdot dz \cdot W/(r \text{ of } AA_1). \tag{17}$$

Also,

$$r(\text{of } EA) = 6 \cdot (r \text{ of } AA_1)$$

while

$$r(\text{of } FA) = 0.86 \cdot H \cdot (1 - 1.2\,\delta/H) \quad \text{for } r > tH/7 \tag{18}$$

otherwise

$$r = t \cdot H/7$$

$$dW(\text{at } EA) = 8 \cdot M_P \cdot EB \cdot dz/(r \text{ of } EA) \tag{19}$$

and

$$dW(\text{at } FA) = 8 \cdot M_P \cdot EB \cdot dz/(r \text{ of } FA) \tag{20}$$

$$\alpha_{KK} = \sin^{-1}[z/(H-z)] \tag{21}$$

and

$$W_{KK} = 2 \cdot M_P \cdot (W + 2 \cdot a \cdot H) \cdot \alpha_{KK}. \tag{22}$$

Since all the energy is absorbed by plastic deformation along the hinge lines of the collapse mechanism, the total value of the energy absorbed may be obtained by summing up the above equations. The load $P(\delta)$ at any δ is then calculated numerically as follows:

$$P(\delta) = [W(\delta + \Delta\delta) - W(\delta)]/\Delta\delta. \tag{23}$$

Figures 10(a) and (b) show typical experimental and theoretical load compression results for 24 mm and 35 mm aluminium tubes respectively, when compressed under a 24 mm wide flat-faced indenter. Corresponding energy curves are shown in Fig. 11. Figures 12 and 13 compare such results for 24 mm and 37 mm steel tubes respectively. These curves are for the flat-faced indenters of 4 mm and 24 mm width.

The experimental and theoretical results when compared in general show that theoretical curves fall gradually and continuously in the post collapse region. The analysis however gives a fair approximation of the tube behaviour, because the rise in the experimental curves occurs at a stage when the tube ends begin to press against the opposite platen. This effect, however, is ignored in the analysis and therefore the theoretical curves tend to drop continuously.

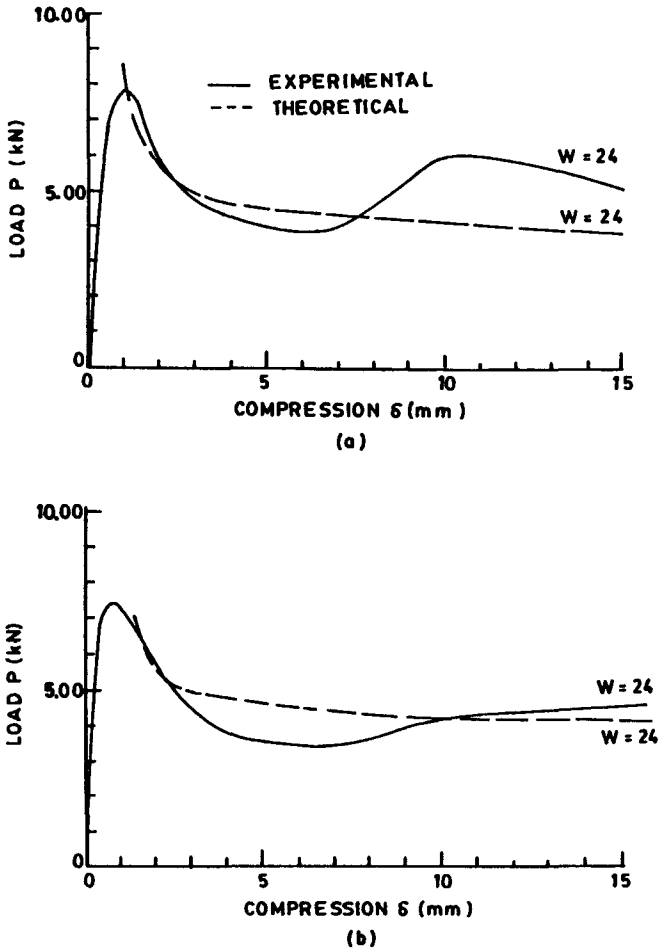

Fig. 10. Theoretical and experimental load compression curves for (a) 24 mm and (b) 35 mm aluminium tubes, under 24 mm flat.

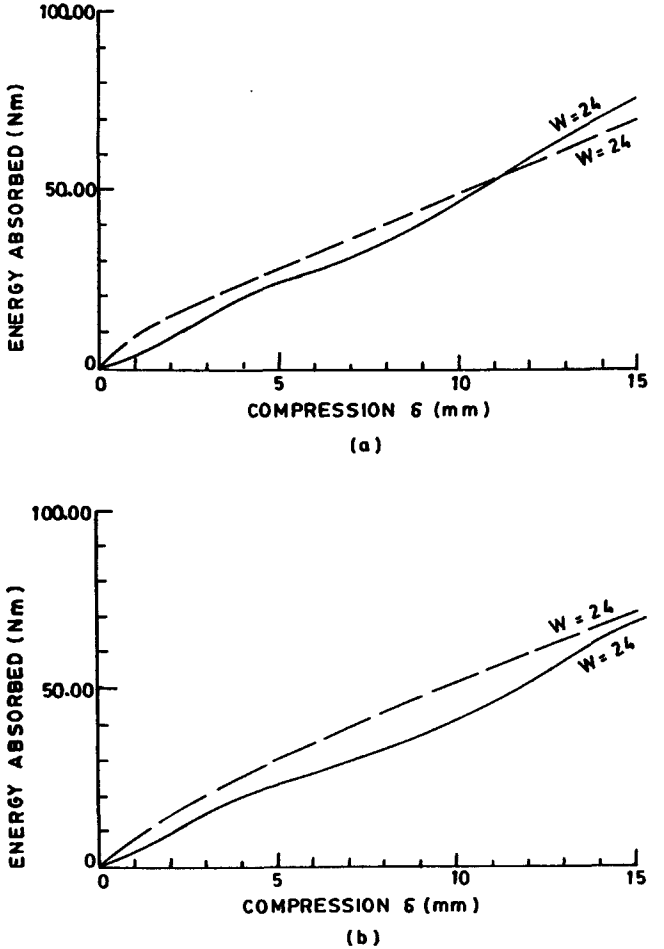

Fig. 11. Theoretical and experimental curves of energy absorbed vs compression for (a) 24 mm, (b) 35 mm aluminium tubes under 24 mm wide platen.

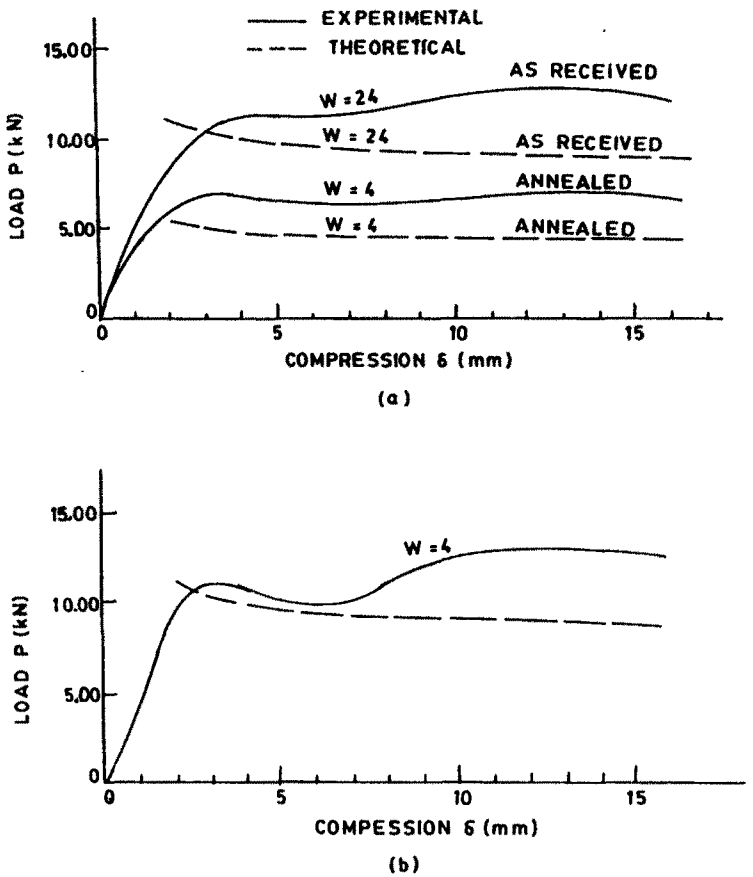

Fig. 12. Theoretical and experimental load compression curves for (a) 24 mm and (b) 37 mm steel tubes. Indenter width is indicated on each curve.

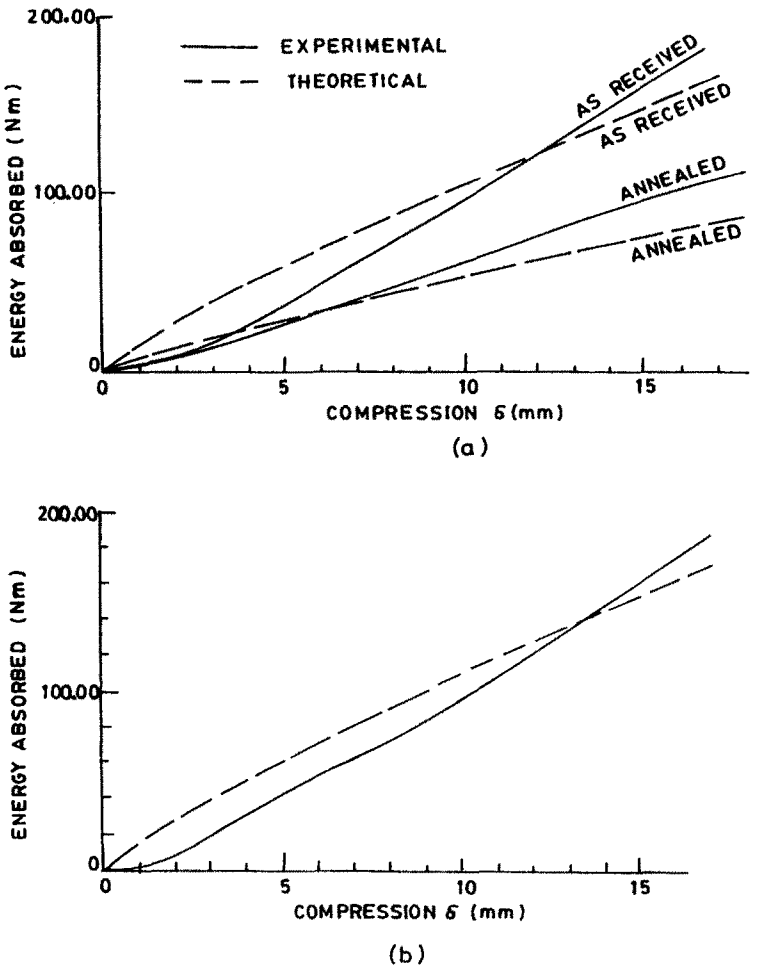

Fig. 13. Theoretical and experimental curves of energy absorbed vs compression for (a) 24 mm and (b) 37 mm steel tubes.

5. CONCLUSIONS

Experiments on lateral compression of a tube between a wedge-shaped or a flat-faced indenter and a flat base reveal that its deformation and the load compression curve are dependent on the tube length and the indenter angle or its width. As long as the tube length is short, see Fig. 7(a), the load compression curve drops continuously and the peak load rises almost linearly with the length of the tube. For sufficient overhangs (>1.5–$2H$) on either side of the indenter, however, the peak load variations become negligible for a given indenter. The load compression curve in this case, shows a second rise of load when the tube ends, which are bending inwards, begin to press against the opposite platen of the machine. The analysis presented here is valid for sufficient overhang but does not consider this pressing of the tube ends against the opposite platen. The results thus obtained compare well with the experiments up to this.

REFERENCES

Ezra, A. A. and Fay, R. J. (1972). An assessment of energy absorbing devices for prospective use in aircraft impact situations. In *Dynamic Response of Structures* (Edited by G. Herrman and N. Perrone), pp. 225–246. Pergamon Press, Oxford.

Gupta, N. K. and Sinha, S. K. (1989). Transverse Collapse of Square Tubes. Thin Walled Structures (Communicated).

Johnson, W. and Reid, S. R. (1978). Metallic energy dissipating system. *App. Mech. Rev.* **31**(3), 277–288.

Jones, N. and Abramowicz, W. (1985). Static and dynamic axial crushing of circular and square tubes. In *Metal Forming and Impact Mechanics* (Edited by S. R. Reid), pp. 225–247. Pergamon Press, Oxford.

Meng, Q., Al-Hasani, S. T. S. and Soden, P. D. (1983). Axial crushing of square tubes. *Int. J. Mech. Sci.* **25**, 747–773.

Reid, S. R. (1983). Laterally compressed metal tubes as impact energy absorbers. In *Structural Crashworthiness* (Edited by N. Jones and T. Wierzbicki), pp. 1–43. Butterworth, London.

Sinha, D. K. and Chitkara, N. R. (1982). Plastic collapse of square rings. *Int. J. Solids Structures* **18**(9), 819–826.

Sinha, D. K. and Chitkara, N. R. (1982). A simplified solution for plastic collapse loads of square tubes subjected to opposed transverse line loads. *Acta Mechanica* **44**(3–4), 177.

Sinha, S. K. (1988). *Lateral Compression of Square Tubes and Their Cross Layered Systems*. Ph.D. Thesis, Indian Institute of Technology, Delhi.